

# Zee model and phenomenology of lepton sector

EIICHI MITSUDA AND KEN SASAKI\*

*Dept. of Physics, Faculty of Engineering, Yokohama National University  
Yokohama 240-8501, JAPAN*

## Abstract

The virtual effects of the Zee charged scalar boson on the lepton-family-number (LFN) violating processes are studied. We obtain the constraints on the individual Yukawa coupling constants of the Zee boson to leptons. Using these constraints, we predict the upper bounds on the muonium-antimuonium conversion probability, the branching fractions of the LFN violating decays such as  $\tau \rightarrow e\gamma$ ,  $\tau \rightarrow \mu\gamma$ ,  $\tau^- \rightarrow \mu^+e^-e^-$  and  $\tau \rightarrow e^+\mu^-\mu^-$ . The contribution of the Zee boson to the muon anomalous magnetic moment is also considered.

PACS: 12.60.-i; 13.15.+g; 13.35.-r

---

\*e-mail address: sasaki@phys.ynu.ac.jp

Accumulated data on atmospheric, solar and accelerator neutrino experiments indicate that neutrinos have small but finite masses and mix among flavors [1]. Existence of massive neutrinos, even though they are very tiny, necessitates the extension of the standard model (SM) for electroweak interactions. To explain the smallness of neutrino masses, there are two well-known mechanisms. One is the see-saw mechanism which introduces heavy right-handed Majorana neutrinos [2]. The other is the radiative mechanism in which neutrino masses are generated by radiative corrections and the left-handed neutrinos acquire the Majorana masses. The simplest model for the latter scenario was presented by Zee [3]. In this model, the ordinary left-handed neutrinos are employed while a new charged scalar field  $h$ , being a  $SU(2)_L$  singlet, and two doublets of Higgs bosons  $\Phi_1, \Phi_2$  are introduced. The neutrino mass matrix in the Zee model, generated at one-loop level, shows a very distinctive pattern [4, 5]. Recently, in connection with neutrino oscillations, the neutrino mass and mixing matrices of the Zee model have been extensively studied [6, 7]. Especially, it has been recognized [7] that the Zee model yields a solution for the bi-maximal neutrino mixing both in atmospheric and solar neutrino oscillations [8].

The charged scalar boson  $h$  in the Zee model carries lepton number  $L(= L_e + L_\mu + L_\tau) = 2$ , and its Yukawa couplings to leptons violate the lepton-family-number (LFN) conservation. Thus the Zee scalar boson  $h$  not only plays a crucial role for neutrino mass generation, but also it induces other interesting LFN violating weak processes. In fact, these processes have been studied before in the Zee model and some constraints on the Yukawa couplings between the Zee boson  $h$  and leptons have been obtained [3]-[6],[9]-[11].

In this paper we further study the virtual effects of the Zee boson on the LFN violating weak processes. Although some information on the parameters in the Zee model has been reported from the analysis of neutrino oscillations within the framework of the Zee mass matrix [7], we refrain from its use here. Instead, we employ the experimental upper bounds on the muon decay rate, the  $g_\mu/g_e$  ratio, and the  $\mu \rightarrow e\gamma$  branching fraction, and show that we can obtain the constraints on the individual ratios,  $\frac{|f_{e\mu}|^2}{M_1^2}$ ,  $\frac{|f_{e\tau}|^2}{M_1^2}$ , and  $\frac{|f_{\mu\tau}|^2}{M_1^2}$ , where  $f_{ij}$ 's are the Yukawa coupling

constants of the Zee boson  $h$  to leptons and  $\overline{M}_1$  is the ‘‘Zee boson’’ mass (see Eq.(7) below for the definition). With these constraints at hand, we analyze other LFN violating processes such as the muonium-antimuonium conversion,  $\tau \rightarrow e\gamma$ ,  $\tau \rightarrow \mu\gamma$ ,  $\tau^- \rightarrow \mu^+e^-e^-$  and  $\tau \rightarrow e^+\mu^-\mu^-$  decays. Finally we consider the contribution of the Zee boson to the muon anomalous magnetic moment.

In the Zee model, the following Lagrangian is added to the SM:

$$\begin{aligned}
\mathcal{L}_{\text{Zee}} &= \sum_{i,j=e,\mu,\tau} f_{ij} \psi_{iL}^T C(i\sigma_2) \psi_{jL} h^+ + \mu \Phi_1^T (i\sigma_2) \Phi_2 h^- + h.c. \\
&= 2f_{e\mu} [\nu_{eL}^T C \mu_L - e_L^T C \nu_{\mu L}] h^+ + 2f_{e\tau} [\nu_{eL}^T C \tau_L - e_L^T C \nu_{\tau L}] h^+ \\
&+ 2f_{\mu\tau} [\nu_{\mu L}^T C \tau_L - \mu_L^T C \nu_{\tau L}] h^+ + \mu (\Phi_1^+ \Phi_2^0 - \Phi_1^0 \Phi_2^+) h^- + h.c. , \quad (1)
\end{aligned}$$

where  $\psi_{iL} = (\nu_i, l_i)_L^T$  (with  $i$  a family index) is an usual left-handed lepton doublet and  $h^\pm$  is the  $SU(2)_L$  singlet Zee scalar boson. Two Higgs doublets,  $\Phi_j = (\Phi_j^+, \Phi_j^0)^T, j = 1, 2$ , are introduced and we assume that only  $\Phi_1$  couples to leptons. Since  $f_{ij}$  is antisymmetric under the interchange of lepton family indices  $i$  and  $j$ , the Yukawa couplings of  $h$  to leptons violate the lepton-*family*-number-conservation. After the neutral components having acquired the vacuum expectation values,  $\langle \Phi_j^0 \rangle = v_j/\sqrt{2}$ , the charged Higgs boson (which is orthogonal to the would-be Goldstone boson) is expressed as

$$\Phi^+ = \cos\beta \Phi_1^+ - \sin\beta \Phi_2^+ , \quad (2)$$

where  $\tan\beta \equiv \frac{v_1}{v_2}$ . This charged Higgs boson  $\Phi^+$  mixes with the Zee boson  $h^+$  due to the  $\Phi_1$ - $\Phi_2$ - $h$  interaction given in Eq.(1). After the charged scalar mass matrix being diagonalized,  $h^+$  and  $\Phi^+$  are expressed in terms of the physical charged scalar bosons  $H_1^+$  and  $H_2^+$  with mass eigenvalues  $M_1^2$  and  $M_2^2$ , respectively, as [5]

$$\begin{pmatrix} h^+ \\ \Phi^+ \end{pmatrix} = \begin{pmatrix} \cos\phi & \sin\phi \\ -\sin\phi & \cos\phi \end{pmatrix} \begin{pmatrix} H_1^+ \\ H_2^+ \end{pmatrix} , \quad (3)$$

with

$$\sin 2\phi = \frac{2\sqrt{2}\mu M_W}{g(M_1^2 - M_2^2)} , \quad (4)$$

where  $M_W = \frac{g}{2}\sqrt{v_1^2 + v_2^2}$ , the mass of  $W$  gauge boson, and  $g$  is the  $SU(2)_L$  gauge coupling constant.

Since the physical charged  $H_1^\pm$  and  $H_2^\pm$  bosons are a linear combination of  $h^\pm$  and  $\Phi^\pm$ , the interaction of  $H_1$  and  $H_2$  with leptons is made up of two parts, one being LFN conserving and the other LFN changing, and it takes the following form:

$$\begin{aligned} \mathcal{L}^{\text{lepton}-H_i} = & \frac{g \cot \beta}{\sqrt{2} M_W} \left( \sum_{i=e,\mu,\tau} m_i \bar{\nu}_{iL} l_{iR} \right) \left( -\sin \phi H_1^+ + \cos \phi H_2^+ \right) \\ & + \left\{ 2f_{e\mu} \left[ \nu_{eL}^T C \mu_L - e_L^T C \nu_{\mu L} \right] + 2f_{e\tau} \left[ \nu_{eL}^T C \tau_L - e_L^T C \nu_{\tau L} \right] \right. \\ & \left. + 2f_{\mu\tau} \left[ \nu_{\mu L}^T C \tau_L - \mu_L^T C \nu_{\tau L} \right] \right\} \left( \cos \phi H_1^+ + \sin \phi H_2^+ \right) + h.c. . \quad (5) \end{aligned}$$

The terms in the first line are LFN conserving and each term is proportional to a lepton mass  $m_i$ , and the rest are LFN changing terms stemming from the  $h^\pm$ -lepton interactions.

The effective four-fermion Lagrangian induced by  $H_1$  and  $H_2$  exchange gives observable contributions to weak processes. The dominant terms for the decays  $\mu \rightarrow e \bar{\nu} \nu$ ,  $\tau \rightarrow e \bar{\nu} \nu$ , and  $\tau \rightarrow \mu \bar{\nu} \nu$ , for example, are given by [6, 11]

$$\begin{aligned} -\mathcal{L}_{\text{eff}} = & \frac{4G_F}{\sqrt{2}} \left\{ \left( 1 + \frac{|f_{e\mu}|^2}{\sqrt{2} G_F \overline{M}_1^2} \right) \left[ \bar{e}_L \gamma_\lambda \nu_{eL} \right] \left[ \bar{\nu}_{\mu L} \gamma^\lambda \mu_L \right] \right. \\ & + \left( 1 + \frac{|f_{e\tau}|^2}{\sqrt{2} G_F \overline{M}_1^2} \right) \left[ \bar{e}_L \gamma_\lambda \nu_{eL} \right] \left[ \bar{\nu}_{\tau L} \gamma^\lambda \tau_L \right] \\ & \left. + \left( 1 + \frac{|f_{\mu\tau}|^2}{\sqrt{2} G_F \overline{M}_1^2} \right) \left[ \bar{\mu}_L \gamma_\lambda \nu_{\mu L} \right] \left[ \bar{\nu}_{\tau L} \gamma^\lambda \tau_L \right] \right\} , \quad (6) \end{aligned}$$

where

$$\frac{1}{\overline{M}_1^2} = \frac{\cos^2 \phi}{M_1^2} + \frac{\sin^2 \phi}{M_2^2} . \quad (7)$$

The constraint on  $|f_{e\mu}|^2/\overline{M}_1^2$  has been obtained from the study of the muon decay rate. Smirnov and Tanimoto [6] got  $|f_{e\mu}|^2/\overline{M}_1^2 < 7 \times 10^{-4} G_F$  by assuming that the effect of the new bosons on the muon decay rate is smaller than 0.1%. On the other hand, McLaughlin and Ng [11] obtained

$$\frac{|f_{e\mu}|^2}{\overline{M}_1^2} < 3 \times 10^{-3} G_F , \quad (8)$$

by demanding that the corrections be no bigger than the error of the SM Fermi constant. In this paper we take the latter one, a rather conservative constraint for  $|f_{e\mu}|^2/\overline{M}_1^2$ . Authors of Ref.[11] also pointed out that an information on the difference  $(|f_{e\tau}|^2 - |f_{\mu\tau}|^2)/\overline{M}_1^2$  can be obtained from the ratio of  $\tau$  decay rates  $\Gamma(\tau \rightarrow \mu\bar{\nu}\nu)/\Gamma(\tau \rightarrow e\bar{\nu}\nu)$ . Quite recently new results have been reported on the branching fractions of  $\tau$  into leptons [12] and the ratio of the charged current coupling constants of the muon and electron is determined to be  $g_\mu/g_e = 1.0007 \pm 0.0051$ . The Zee model predicts (see Eq.(6)),

$$\frac{g_\mu}{g_e} = 1 + \frac{1}{\sqrt{2}G_F} \frac{|f_{\mu\tau}|^2 - |f_{e\tau}|^2}{\overline{M}_1^2}. \quad (9)$$

Taking the bound  $|\frac{g_\mu}{g_e} - 1| < 0.006$ , we obtain

$$\left| \frac{|f_{\mu\tau}|^2}{\overline{M}_1^2} - \frac{|f_{e\tau}|^2}{\overline{M}_1^2} \right| < 8.5 \times 10^{-3} G_F. \quad (10)$$

This gives only the upper bound on the difference. However, if we combine this constraint with the one from the  $\mu \rightarrow e\gamma$  decay, we obtain the individual bounds on  $|f_{\mu\tau}|^2/\overline{M}_1^2$  and  $|f_{e\tau}|^2/\overline{M}_1^2$ . In the Zee model, the branching fraction for  $\mu \rightarrow e\gamma$  is given by [5]

$$B(\mu \rightarrow e\gamma) = \frac{\alpha}{48\pi} \left( \frac{|f_{\mu\tau}f_{e\tau}|}{G_F\overline{M}_1^2} \right)^2. \quad (11)$$

The present experimental upper bound,  $B(\mu \rightarrow e\gamma) < 1.2 \times 10^{-11}$  [16], leads to

$$\frac{|f_{\mu\tau}f_{e\tau}|}{\overline{M}_1^2} < 2.8 \times 10^{-4} G_F. \quad (12)$$

Then we find that the above constraint, combined with Eq.(10), gives the bounds

$$\frac{|f_{\mu\tau}|^2}{\overline{M}_1^2}, \quad \frac{|f_{e\tau}|^2}{\overline{M}_1^2} < 8.5 \times 10^{-3} G_F. \quad (13)$$

The fact that  $|f_{\mu\tau}|^2/\overline{M}_1^2$  and  $|f_{e\tau}|^2/\overline{M}_1^2$  individually get almost the same bound as their difference is due to the very stringent constraint of Eq.(12). Of course, if we get more precise determination of the  $g_\mu/g_e$  ratio, we can set more stringent bounds on  $|f_{\mu\tau}|^2/\overline{M}_1^2$  and  $|f_{e\tau}|^2/\overline{M}_1^2$ .

With these bounds on the Yukawa coupling constants  $f_{ij}$ , Eqs.(8), (12), (13), we now discuss the weak processes involving charged  $H_1$  and  $H_2$  bosons. In particular we are interested in the LFN violating processes.

*The muonium-antimuonium conversion.* In the Zee model, the mixing of muonium  $M(\mu^+e^-)$  and antimuonium  $\bar{M}(\mu^-e^+)$  arises, at one-loop-level, only through one diagram, the one with two  $H_i$  exchange illustrated in Fig.1(a). Using a formula for the loop integral

$$\begin{aligned} i \int \frac{d^4k}{(2\pi)^4} \frac{1}{k^2 - M_i^2} \frac{1}{k^2 - M_j^2} \left[ \frac{1}{\not{k}} \right] \left[ \frac{1}{\not{k}} \right] &= \frac{1}{64\pi^2} \frac{1}{M_i^2 - M_j^2} \ln \frac{M_i^2}{M_j^2} [\gamma_\lambda] [\gamma^\lambda] \quad (i \neq j), \\ &= \frac{1}{64\pi^2} \frac{1}{M_i^2} [\gamma_\lambda] [\gamma^\lambda] \quad (i = j), \end{aligned}$$

where  $[1/\not{k}]$  is coming from the internal neutrino propagator, we obtain the following effective Lagrangian for the  $M$ - $\bar{M}$  conversion:

$$-\mathcal{L}_{\text{eff}}^{M\bar{M}} = \frac{G_{M\bar{M}}}{\sqrt{2}} [\bar{\mu}\gamma_\lambda(1 - \gamma_5)e] [\bar{\mu}\gamma^\lambda(1 - \gamma_5)e], \quad (14)$$

with

$$\frac{G_{M\bar{M}}}{\sqrt{2}} = \frac{|f_{e\tau}f_{\mu\tau}|^2}{16\pi^2} \frac{1}{\widetilde{M}^2}, \quad (15)$$

where

$$\frac{1}{\widetilde{M}^2} = \frac{\cos^4\phi}{M_1^2} + \frac{2\cos^2\phi \sin^2\phi}{M_1^2 - M_2^2} \ln \frac{M_1^2}{M_2^2} + \frac{\sin^4\phi}{M_2^2}. \quad (16)$$

Note that  $\mathcal{L}_{\text{eff}}^{M\bar{M}}$  is in the  $(V - A) \times (V - A)$  form<sup>1</sup>. The integrated probability that the muonium  $M(\mu^+e^-)$  decays as  $\mu^-$  rather than  $\mu^+$  is given by [14]

$$P(\bar{M}) = 64G_{M\bar{M}}^2/\pi^2 a_B^6 \lambda^2, \quad (17)$$

where  $a_B$  is the Bohr radius  $(m_e\alpha)^{-1}$  and  $\lambda = G_F^2 m_\mu^5/192\pi^3$  is the muon decay rate. Using the bound (12) and the relation

$$\frac{1}{\widetilde{M}^2} \leq \frac{1}{M_1^2} \quad \text{for arbitrary } \phi, \quad (18)$$

---

<sup>1</sup>The  $M$ - $\bar{M}$  conversion experiments have been performed under the influence of external magnetic field. The  $M$ - $\bar{M}$  conversion probability reduces with the applied magnetic field, and the reduction depends on the effective Hamiltonian being in the form of  $(V \mp A) \times (V \mp A)$ , or  $(V \mp A) \times (V \pm A)$  or other interaction types [13]

(the equality holds when  $M_1^2 = M_2^2$ ), we obtain

$$P(\overline{M}) < 9.5 \times 10^{-24} \left[ \frac{\overline{M}_1^2}{M_W^2} \right]^2 . \quad (19)$$

For  $\overline{M}_1 = 800$  GeV, we get  $P(\overline{M}) < 10^{-19}$ . The present experimental upper limit [15] is  $P(\overline{M}) < 2.4 \times 10^{-10}$  (90% C.L.).

In fact, the muonium-antimuonium oscillation was studied before in the Zee model and the same box diagram in Fig.1(a) was analyzed [9, 10]. But our result on the effective Lagrangian for the muonium-antimuonium conversion disagrees with the one given in Ref.[9, 10], in respect to its chiral structure and magnitude. Comparing with Eqs.(4.116-117) of Ref.[10], we find that our result on  $\frac{G_{\overline{M}}}{\sqrt{2}}$  in Eq.(15) is without a suppression factor  $(m_\mu/\mu_S)^2$ , where  $\mu_S$  is the charged Zee boson mass introduced there, expected to be the same order of magnitude as our  $\overline{M}_1$ .

*The  $\tau \rightarrow e\gamma$  and  $\tau \rightarrow \mu\gamma$  decays.* With replacement of  $f_{\mu\tau}f_{e\tau}$  in Eq.(11) with appropriate  $f_{ij}$ , the branching fractions for both decays are given by

$$B(\tau \rightarrow e\gamma) = \frac{\alpha}{48\pi} \left[ \frac{|f_{e\mu}f_{\mu\tau}|}{G_F \overline{M}_1^2} \right]^2 B(\tau \rightarrow e\overline{\nu}_e\nu_\tau) , \quad (20)$$

$$B(\tau \rightarrow \mu\gamma) = \frac{\alpha}{48\pi} \left[ \frac{|f_{e\mu}f_{e\tau}|}{G_F \overline{M}_1^2} \right]^2 B(\tau \rightarrow e\overline{\nu}_e\nu_\tau) . \quad (21)$$

The constraints (8), (13) and  $B(\tau \rightarrow e\overline{\nu}_e\nu_\tau)_{\text{exp}} = (17.83 \pm 0.06)\%$  [16] lead to

$$B(\tau \rightarrow e\gamma) , \quad B(\tau \rightarrow \mu\gamma) < 2.0 \times 10^{-10} , \quad (22)$$

both being far below the present experimental upper bounds ( $\sim 10^{-6}$ ) [16].

*The  $\tau^- \rightarrow \mu^+e^-e^-$  and  $\tau \rightarrow e^+\mu^-\mu^-$  decays.* The decay  $\tau^- \rightarrow \mu^+e^-e^-$  arises, at one-loop level, from the diagram with two  $H_i$  boson exchange depicted in Fig.1(b). The loop integral gives

$$\mathcal{L}^{\tau \rightarrow \mu ee} = \frac{C^{\tau \rightarrow \mu ee}}{\sqrt{2}} \left[ \overline{e}\gamma_\lambda(1 - \gamma_5)\tau \right] \left[ \overline{e}\gamma^\lambda(1 - \gamma_5)\mu \right] , \quad (23)$$

with

$$\frac{C^{\tau \rightarrow \mu ee}}{\sqrt{2}} = \frac{f_{\mu\tau}^* f_{e\tau} f_{e\mu}}{16\pi^2} \frac{1}{\overline{M}^2} . \quad (24)$$

Keeping in mind the antisymmetrization of the final two identical electrons and a symmetry factor  $\frac{1}{2}$ , and neglecting the muon and electron masses, we obtain,  $\Gamma(\tau^- \rightarrow \mu^+ e^- e^-) = |C^{\tau \rightarrow \mu ee}|^2 m_\tau^5 / 96\pi^3$ , for the decay rate. Then we get the upper limit on the branching fraction of the  $\tau^- \rightarrow \mu^+ e^- e^-$  decay,

$$B(\tau^- \rightarrow \mu^+ e^- e^-) < 2 \times 10^{-18} \left[ \frac{\overline{M}_1}{M_W^2} \right]^2. \quad (25)$$

Similarly, the contribution to the decay  $\tau \rightarrow e^+ \mu^- \mu^-$  comes from the one-loop diagram in Fig.1(c). Now the coefficient  $C^{\tau \rightarrow \mu ee} / \sqrt{2}$  in Eq.(24) is replaced with  $C^{\tau \rightarrow e \mu \mu} / \sqrt{2} = f_{e\tau}^* f_{\mu\tau} f_{e\mu} / 16\pi^2 \widetilde{M}^2$ , and we obtain the same upper limit on  $B(\tau^- \rightarrow e^+ \mu^- \mu^-)$  as the  $\tau^- \rightarrow \mu^+ e^- e^-$  decay. For  $\overline{M}_1 = 800$  GeV, we get the bound  $2 \times 10^{-14}$  for the branching fractions of both decays. The present experimental upper limits on both decays are  $B_{\text{exp}} < 1.5 \times 10^{-6}$  (90% C.L.) [16].

*The  $\mu \rightarrow 3e$  decay.* This process is possible in all models which allow the  $\mu \rightarrow e\gamma$ . The photon is now virtual and decays into a  $e^+ e^-$  pair. Contributions of the  $Z$  boson-exchange graphs instead of photon are negligible. Thus the branching ratio has been estimated to be  $B(\mu \rightarrow 3e) \approx (\alpha/\pi) B(\mu \rightarrow e\gamma)$  [5]. At one-loop level in the Zee model, there is another diagram contributing to the decay  $\mu \rightarrow 3e$ , a box diagram resembling the ones in Fig.1 with two  $H_i$  exchange.<sup>2</sup> The diagram gives

$$- \mathcal{L}_{\text{box}}^{\mu \rightarrow 3e} = \frac{C_{\text{box}}^{\mu \rightarrow 3e}}{\sqrt{2}} \left[ \bar{e} \gamma_\lambda (1 - \gamma_5) \mu \right] \left[ \bar{e} \gamma^\lambda (1 - \gamma_5) e \right], \quad (26)$$

with

$$\frac{C_{\text{box}}^{\mu \rightarrow 3e}}{\sqrt{2}} = \frac{f_{e\tau} f_{\mu\tau}^*}{16\pi^2} \left[ |f_{e\mu}|^2 + |f_{e\tau}|^2 \right] \frac{1}{\widetilde{M}^2}. \quad (27)$$

Assuming that this box diagram contribution adds to the decay rate incoherently, we obtain the ratio

$$\frac{\Gamma(\mu \rightarrow 3e)_{\text{box}}}{\Gamma(\mu \rightarrow e\gamma) \frac{\alpha}{\pi}} = 12 \left[ \frac{|f_{e\mu}|^2 + |f_{e\tau}|^2}{4\pi\alpha} \right]^2 \left( \frac{\overline{M}_1}{\widetilde{M}} \right)^4. \quad (28)$$

For  $\overline{M}_1 = 800$  GeV, the constraints (8) and (13) give  $|f_{e\mu}|^2 < 0.02$  and  $|f_{e\tau}|^2 < 0.06$ , respectively. Thus, in case  $\overline{M}_1 \sim \widetilde{M}$ , there remains a possibility that this box

<sup>2</sup>The  $\mu \rightarrow 3e$  decay was studied before in the Zee model [9, 10], but our result on  $C_{\text{box}}^{\mu \rightarrow 3e}$  disagree with the one in Refs.[9, 10], which has further a suppression factor  $(m_\mu/\mu_S)^2$ .



diagram contribution to the decay rate  $\mu \rightarrow 3e$  becomes comparable to the one from the photon exchange graph.

The same remarks can be made for such  $\tau$  decays as  $\tau \rightarrow 3e$ ,  $\tau^- \rightarrow e^- \mu^+ \mu^-$ ,  $\tau \rightarrow 3\mu$ , and  $\tau^- \rightarrow \mu^- e^+ e^-$ . The branching fractions for the first two decays are expected to be of the order of  $(\alpha/\pi)B(\tau \rightarrow e\gamma)$  and those for the latter two are  $(\alpha/\pi)B(\tau \rightarrow \mu\gamma)$ . In the Zee model, the two  $H_i$  exchange diagrams also contribute to these LFN violating decays, and their contributions may possibly be comparable to those from the photon exchange diagrams.

*The muon anomalous magnetic moment.* With improvement in the measurement, the anomalous magnetic moment of the muon,  $a_\mu = (g-2)/2$ , has become to provide an excellent laboratory for testing various electroweak gauge models. Quite recently, the new experimental result on the positive muon anomalous magnetic moment was reported [18] and it shows a clear difference between the weighted mean of the experimental results and the SM prediction:

$$a_\mu(\text{exp}) - a_\mu(\text{SM}) = 43(16) \times 10^{-10} . \quad (29)$$

In the Zee model, two new charged scalar mesons  $H_1$  and  $H_2$  appear. We now discuss their contribution to the muon anomalous magnetic moment. There are two relevant diagrams in one loop, which are depicted in Fig.2. The arrows on the fermion lines indicate the flow of lepton number. The diagram in Fig.2(a) is LFN conserving and thus the factor  $(m_\mu/M_W)^2$  appears, while the one in Fig.2(b) is LFN changing and its contribution is proportional to  $|f_{e\mu}|^2 (|f_{\mu\tau}|^2)$ . The calculation is straightforward [17], and we find

$$a_\mu^{(a)} = \frac{m_\mu^4}{24\pi^2} \frac{g^2 \cot^2 \beta}{8M_W^2} \frac{1}{\overline{M}_2^2} , \quad (30)$$

$$a_\mu^{(b)} = \frac{m_\mu^2}{24\pi^2} \frac{|f_{e\mu}|^2 + |f_{\mu\tau}|^2}{\overline{M}_1^2} , \quad (31)$$

where

$$\frac{1}{\overline{M}_2^2} = \frac{\sin^2 \phi}{M_1^2} + \frac{\cos^2 \phi}{M_2^2} . \quad (32)$$

The LFN conserving contribution is rewritten as  $a_\mu^{(a)} = 9 \times 10^{-16} \cot^2 \beta (M_W^2 / \overline{M}_2^2)$ . So even when we take generous values for  $\cot \beta$  and  $\overline{M}_2$ , say,  $\cot \beta \sim 50$  and  $\overline{M}_2 \sim 200$  GeV, we get  $a_\mu^{(a)} \sim 4 \times 10^{-13}$ . For the LFN violating part, the bounds (8) and (13) give  $a_\mu^{(b)} < 6 \times 10^{-12}$ . Thus we observe that the contribution of the charged scalar bosons  $H_1$  and  $H_2$  to the muon anomalous magnetic moment is not sufficient to fill the difference (29). In addition to these charged scalar bosons, there appear three neutral Higgs bosons in the Zee model. But their contributions to the muon anomalous magnetic moment are proportional to  $(m_\mu^2 / M_W M_H)^2$ , where  $M_H$  is a relevant Higgs mass, and, therefore, they are negligible. So we conclude that the Zee model in its original form cannot fill the present gap (29) between the experiment and the SM prediction.

The Zee model is one of the promising candidates which may explain the phenomena of atmospheric and solar neutrino oscillations. Also it predicts many interesting LFN violating weak processes. Gaining the current constraints on the individual Yukawa coupling constants,  $|f_{e\mu}|^2 / \overline{M}_1^2$ ,  $|f_{e\tau}|^2 / \overline{M}_1^2$ , and  $|f_{\mu\tau}|^2 / \overline{M}_1^2$ , in the Zee model, we have studied the virtual effects of the Zee boson on the phenomenology of lepton sector. The predicted effects on the LFN violating weak processes are found to be small and far below the present experimental upper limits. Also it is found that the contribution of the new bosons in the Zee model to the muon anomalous magnetic moment is too small to fill the present difference between the experiment and the SM prediction. If this gap persists, we are compelled to abandon the Zee model or to pursue the extensions of its original form<sup>3</sup>. Embedding the original Zee model into supersymmetry might be one of the most interesting extensions [19].

After submitting the paper, our attention has been called to the following two papers, Ref.[20] and Ref.[21]. In the first reference.[20], an effective field theory has been built by integrating out the heavy scalar in the Zee model. The effective lagrangians obtained for the four-fermi interactions are consistent with our results. In the second reference [21], it was pointed out also that the minimal Zee model cannot resolve the BNL  $g - 2$  anomaly, using the neutrino oscillation data, and the

---

<sup>3</sup>An extension of the Zee model which includes singlet neutrinos has been considered in Ref.[11].

extensions of the Zee model have been considered to explain the mass patterns of the neutrinos and leptons and the BNL  $g - 2$  anomaly.

One of the authors (K.S) would like to thank M. Bando, N. Haba, T. Kugo, and M. Tanimoto for helpful discussions. This work is supported by the Grant-in-Aid for Scientific Research on Priority Areas (A), Ministry of Education, Japan (No. 12047212).

## References

- [1] For a review see M.C. Gonzalez-Garcia, in: Proc. 30th ICHEP Conf., Osaka, July 2000, hep-ph/0010136.
- [2] T. Yanagida, in: O. Sawada, A. Sugamoto (Eds.), Proc. Workshop on Unified Theories and Baryon Number in the Universe, KEK Report No. 79-18, Tukuba, 1979, p. 95; M. Gell-Mann, P. Ramond, R. Slansky, in: P. van Nieuwenhuizen, D. Freedmann (Eds.), Supergravity, North-Holland, Amsterdam, 1979, p. 315.
- [3] A. Zee, Phys. Lett. **B93** (1980) 389; **B161** (1985) 141.
- [4] L. Wolfenstein, Nucl. Phys. **B175** (1980) 93.
- [5] S.T. Petcov, Phys. Lett. **B115** (1982) 401; S.M. Bilenky, S.T. Petcov, Rev. Mod. Phys. **59** (1987) 671.
- [6] A.Yu. Smirnov, M. Tanimoto, Phys. Rev. **D55** (1997) 1665.
- [7] C. Jarlskog, M. Matsuda, S. Skadhauge, M. Tanimoto, Phys. Lett. **B449** (1999) 240; P.H. Frampton, S.L. Glashow, Phys. Lett. **B461** (1999) 95; A.S. Joshipura, S.D. Rindani, Phys. Lett. **B464** (1999) 239; D. Chang, A. Zee, Phys. Rev. **D61** (2000) 071303.
- [8] V. Barger, P. Pakvasa, T.J. Weiler, K. Whisnant, Phys. Lett. **B437** (1998) 107; A. Baltz, A.S. Goldhaber, M. Goldhaber, Phys. Rev. Lett. **58** (1998) 5730; Y. Nomura, T. Yanagida, Phys. Rev. **D59** (1999) 017303; M. Jezabek, Y. Sumino, Phys. Lett. **B440** (1998) 327; R.N. Mohapatra, S. Nussinov, Phys. Lett. **B441** (1998) 299; Q. Shafi, Z. Tavartkiladze, Phys. Lett. **B451** (1999) 129; I. Stancu, D.V. Ahluwalia, Phys. Lett. **B460** (1999) 431; H. Georgi, S.L. Glashow, Phys. Rev. **D61** (2000) 097301.
- [9] G.K. Leontaris, K. Tamvakis, J.D. Vergados, Phys. Lett. **B162** (1985) 153.
- [10] J.D. Vergados, Phys. Rep. **133** (1986) 1.
- [11] G.C. McLaughlin, J.N. Ng, Phys. Lett. **B455** (1999) 224.

- [12] The L3 Collaboration, hep-ex/0102023.
- [13] K. Horikawa, K. Sasaki, Phys. Rev. D**53** (1996) 560; G.G. Wong, W.S. Hou, Phys. Lett. B**357** (1995) 145.
- [14] G. Feinberg, S. Weinberg, Phys. Rev. **123** (1961) 1439.
- [15] L. Willmann et.al., Phys. Rev. Lett. **82** (1999) 49.
- [16] Particle Data Group, Euro. Phys. C**15** (2000) 1.
- [17] J.P. Leveille, Nucl. Phys. B**137** (1978) 63; S.R. Moore, K. Whisnant, B.-L. Young, Phys. Rev. D**31** (1985) 105.
- [18] Muon ( $g - 2$ ) Collaboration, hep-ex/0102017.
- [19] K. Cheung, O.C. Kong, Phys. Rev. D**61** (2000) 113012; N. Haba, M. Matsuda, M. Tanimoto, Phys. Lett. B**478** (2000) 351.
- [20] M. Bilenky, A. Santamaria, Nucl. Phys. B**420** (1994) 47.
- [21] D.A. Dicus, H-J. He, J.N. Ng, hep-ph/0103126.

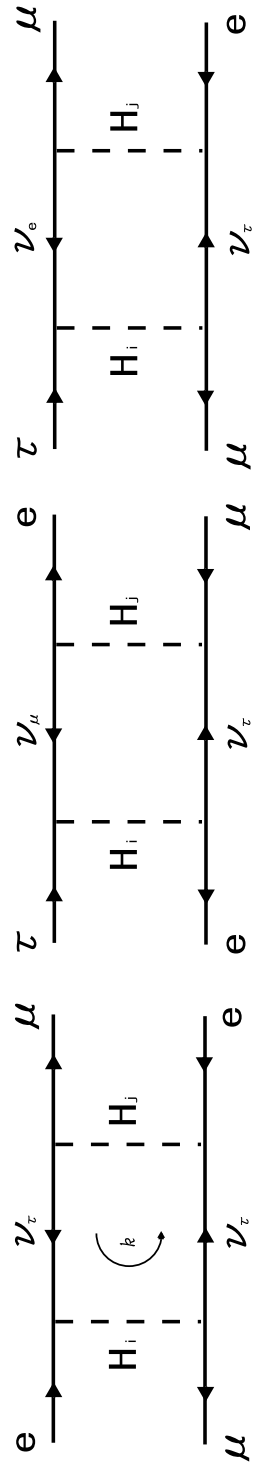
## Figure Caption

Figure 1

The two- $H_i$ -exchange box diagrams relevant for (a) the muonium-antimuonium conversion, (b) the  $\tau \rightarrow \mu^+ e^- e^-$  decay, and (c) the  $\tau \rightarrow e^+ \mu^- \mu^-$  decay. The arrows show the flow of lepton number.

Figure 2

The charged  $H_i$  scalar contributions to  $a_\mu$ : (a) the LFN conserving diagram and (b) the LFN changing diagram. The arrows show the flow of lepton number.



(a)

(b)

(c)

Figure 1

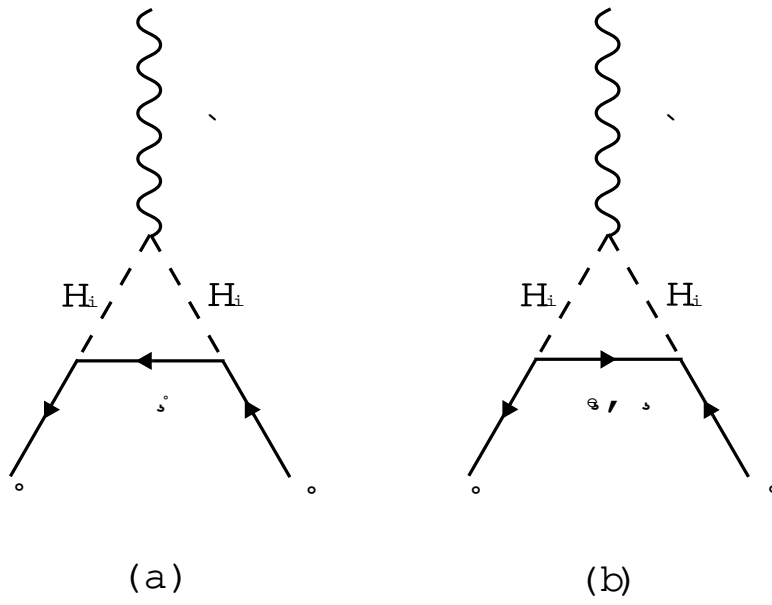


Figure 2